Robust Multifrequency Inversion in Terahertz Tomography

Ke Chen and David Castañón   ECE Department, Boston University

BOSTON UNIVERSITY

Motivation

- **Problem:** The developed joint multifrequency inversion technique outperforms single-frequency inversion, but requires complete and accurate spectral information
- **Goal:** Robust reconstruction approaches which do not assume exact prior information of spectra

Research to reality

This work provides a general framework for robust joint image formation using multiple frequencies for improved reconstruction and sequent recognition. The algorithms are applicable to Terahertz(THz) pulsed imaging which has attracted much attention for its ability to reveal unique spectral characteristics of chemicals in THz range and thus to fingerprint explosives.

Background

Object function:
$o(\boldsymbol{r}, f) = \tilde{n}(\boldsymbol{r}, f)^2 - 1$

Measurement:
$u_s(\boldsymbol{r}) = u(\boldsymbol{r}) - u_0(\boldsymbol{r})$

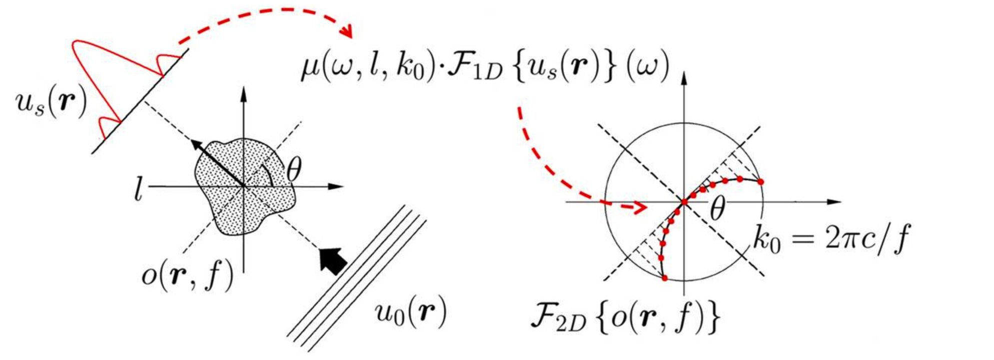

- Fourier Diffraction Theorem[1] relates scattering with object spectrum under the Born approximation $u(\boldsymbol{r}) \approx u_0(\boldsymbol{r})$

$$U_s(\omega_x) = \frac{ie^{il\omega_y}}{2\omega_y} O(\omega_x, \omega_y - k_0),\ \omega_y \triangleq \sqrt{k_0^2 - \omega_x^2}$$

- Model: $\{f_m\}$ in THz radiation spectrum

$$\boldsymbol{y}_m = \boldsymbol{\Psi}_m \boldsymbol{x}_m, \quad m = 1, \ldots, M$$

$\boldsymbol{y}_m \in \mathbb{C}^{K_m}$ Fourier transform(FT) of THz field measurement

$\boldsymbol{x}_m \in \mathbb{C}^N$ Estimate of object function at f_m

$\boldsymbol{\Psi}_m$ Nonuniform FT operator with fast approximation NUFFT[2] $\mathcal{T}_m \approx \boldsymbol{\Psi}_m$

Joint inversion with $\mathcal{E}$

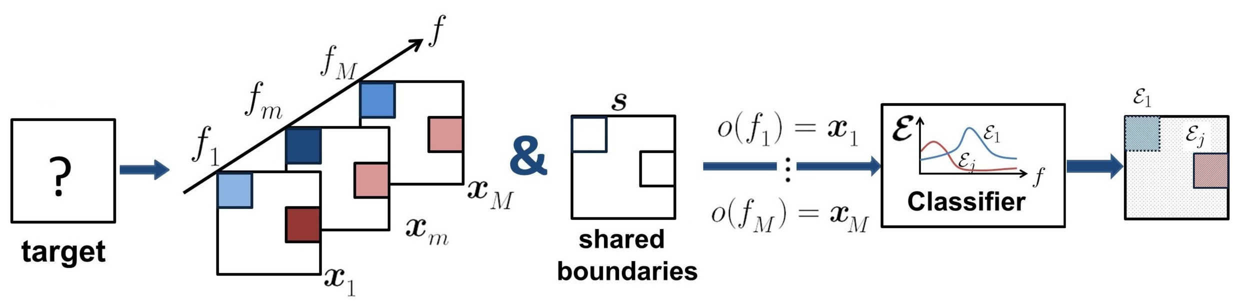

$$\text{JM:} \quad \min_{(\underline{\boldsymbol{x}}, \boldsymbol{s})} \|\underline{\boldsymbol{y}} - \mathcal{T}\underline{\boldsymbol{x}}\|^2 + \alpha_1^2 \|\mathcal{D}^M \underline{\boldsymbol{x}}\|^2_{W^M} + \varphi(\boldsymbol{s}, \gamma)$$

where $\underline{\boldsymbol{x}} = [\boldsymbol{x}_1, \ldots, \boldsymbol{x}_M]^T$, $\mathcal{T} \triangleq \mathrm{diag}[\mathcal{T}_m]$, $W^n := W \otimes \mathbf{I}_n$, derivative operator $\mathcal{D}$

- Data-fidelity term in *frequency* domain, smooth penalty in *spatial* domain
- Jointly construct boundaries $\boldsymbol{s} \in \mathbb{R}^N$: *Invariant* across $\{f_m\}$
- Mumford-Shah[3]: $\varphi(\boldsymbol{s}, \gamma) = \gamma^2 \|\nabla \boldsymbol{s}\|^2 + \frac{1}{\gamma^2}\|\boldsymbol{s}\|^2$

  Spatially varying weighting: $W \triangleq \mathrm{diag}\left[(1 - [\boldsymbol{s}]_i)^2\right]$

Methodologies

Joint inversion with $\mathcal{E}$

$$\text{JMP:} \quad \min_{(\underline{\boldsymbol{\nu}}, \boldsymbol{s})} \|\underline{\boldsymbol{y}} - \mathcal{T}\mathcal{H}\underline{\boldsymbol{\nu}}\|^2 + \alpha_1^2 \|\mathcal{D}^J \underline{\boldsymbol{\nu}}\|^2_{W^J} + \varphi(\boldsymbol{s}, \gamma)$$

where $\underline{\boldsymbol{\nu}} = [\boldsymbol{\nu}_1, \ldots, \boldsymbol{\nu}_J]^T$, $\mathcal{H} = (\mathcal{E}_1 \cdots \mathcal{E}_J) \otimes \mathbf{I}_N$

- Given exact spectral prior $\mathcal{E}_j \in \mathbb{C}^M$, $\quad j = 1, \ldots, J$
- Abundance of the j-th material $\boldsymbol{\nu}_j \in \mathbb{R}^N$, $\quad [\boldsymbol{\nu}_j]_i \in [0, 1]$
- Linear transform[4] $\underline{\boldsymbol{x}} = \mathcal{H}\underline{\boldsymbol{\nu}}$

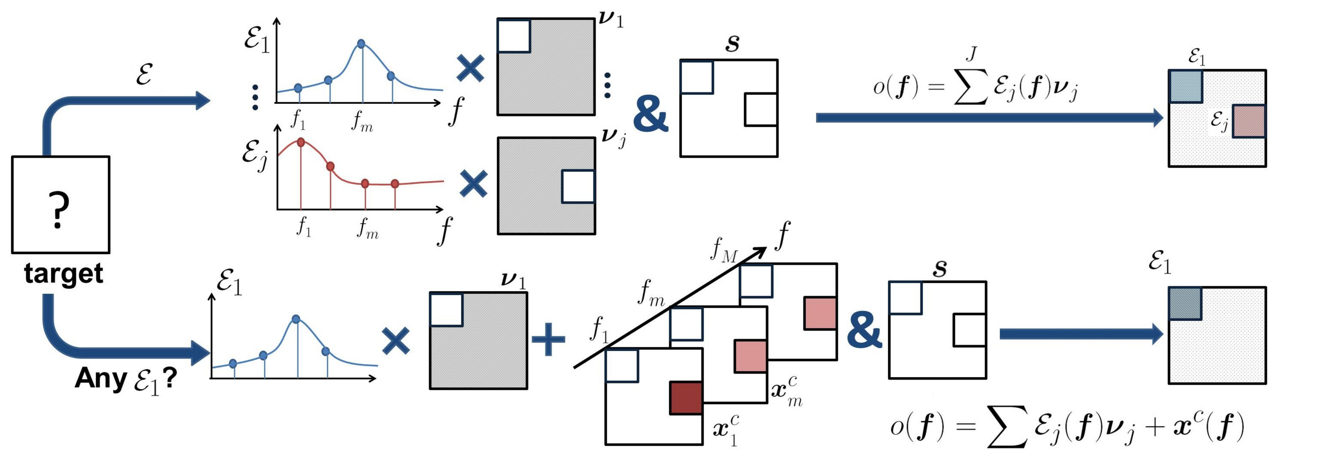

Case 1. With partial $\mathcal{E}$

$$\text{RJMP1:} \quad \min_{(\hat{\underline{\boldsymbol{x}}}, \boldsymbol{s})} \|\underline{\boldsymbol{y}} - \hat{\mathcal{T}}\hat{\underline{\boldsymbol{x}}}\|^2 + \alpha_1^2 \|\mathcal{D}^{(M+J)}\hat{\underline{\boldsymbol{x}}}\|^2_{W^{(M+J)}} + \alpha_2^2 \|\underline{\boldsymbol{x}}^c\|_1^1 + \varphi(\boldsymbol{s}, \gamma)$$

where $\underline{\boldsymbol{x}}^c = [\boldsymbol{x}_1^c, \ldots, \boldsymbol{x}_M^c]^T$, $\hat{\underline{\boldsymbol{x}}} = [\underline{\boldsymbol{\nu}}, \underline{\boldsymbol{x}}^c]^T$, $\hat{\mathcal{T}} = (\mathcal{T}\mathcal{H}, \mathcal{T})$

- Augment $\boldsymbol{x}_m^c \in \mathbb{C}^N$ to compensate prior incomplete
- $\ell_1$norm penalty on $\underline{\boldsymbol{x}}^c$: $\|\boldsymbol{x}\|_1^1 \approx \sum_{i=1}^N \left([\boldsymbol{x}]_i^2 + \beta\right)^{1/2}$

Case 2. With uncertain $\mathcal{E}$

- Uncertainty modelling: $\mathcal{E}_j - \Delta_j \leq \mathbf{e}_j \leq \mathcal{E}_j + \Delta_j$
- Inverse with worst-case prior: $\tilde{\mathcal{H}} = (\mathbf{e}_1 \cdots \mathbf{e}_J) \otimes \mathbf{I}_N$

$$\text{RJMP2:} \quad \min_{(\underline{\boldsymbol{\nu}}, \boldsymbol{s})} \psi(\underline{\boldsymbol{\nu}}, \boldsymbol{s}) + \alpha_1^2 \|\mathcal{D}^J \underline{\boldsymbol{\nu}}\|^2_{W^J} + \varphi(\boldsymbol{s}, \gamma)$$

$$\psi(\underline{\boldsymbol{\nu}}, \boldsymbol{s}) \triangleq \max_{\tilde{\mathcal{H}}} \|\underline{\boldsymbol{y}} - \mathcal{T}\tilde{\mathcal{H}}\underline{\boldsymbol{\nu}}\|^2$$

- NP-hard solving ψ: possible solution $\psi_j(\underline{\boldsymbol{\nu}}, \boldsymbol{s})$ at $\tilde{\mathcal{H}}_j$, $j = 1, \ldots, 2^{2J}$
- Smoothing approximation[5]: $\psi_p(\underline{\boldsymbol{\nu}}, \boldsymbol{s}) \triangleq \lambda^{-1}\log\left(\sum_j \exp(\lambda\psi_j(\underline{\boldsymbol{\nu}}, \boldsymbol{s}))\right)$

References

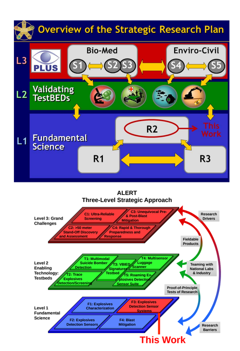

[1] A. Kak, M. Slaney, *Principles of Computerized Tomographic Imaging*, 2001.
[2] J. Fessler, B. Sutton, *IEEE Tr. Sig. Proc.* vol. 51, no. 2, pp. 560-574, 2003.
[3] R. Weisenseel, Ph.D. diss., Boston University, 2004.
[4] A. Li and et al. *Appl. Opt.* vol. 44, no. 10, pp.1948-1956, 2005.
[5] E. Polak and et al. *J Optimiz Theory App* vol. 119, no. 3, 2003.
[6] C. Baker and et al. *Proc. of IEEE* vol.95, no. 8, pp1559-1565, 2007.

This work was supported in part by Gordon-CenSSIS, the Bernard M. Gordon Center for Subsurface Sensing and Imaging Systems, under the Engineering Research Centers Program of the National Science Foundation (Award Number EEC-9986821), and the U.S. Department of Homeland Security (award number 2008-ST-061-ED0001).

Experiment

An 81×81 phantom consisting of 3 explosives and air as background was generated with known spectral prior[6]. We simulated THz incident fields at 19 projection angles, and collected complex amplitude of the scattering at 4 frequencies for reconstruction. Each method was evaluated under various levels of Gaussian noise.

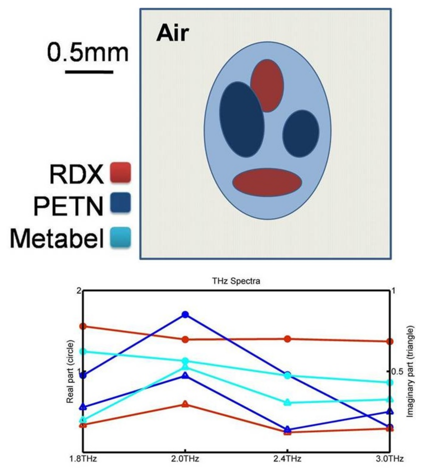

Target and spectrum prior

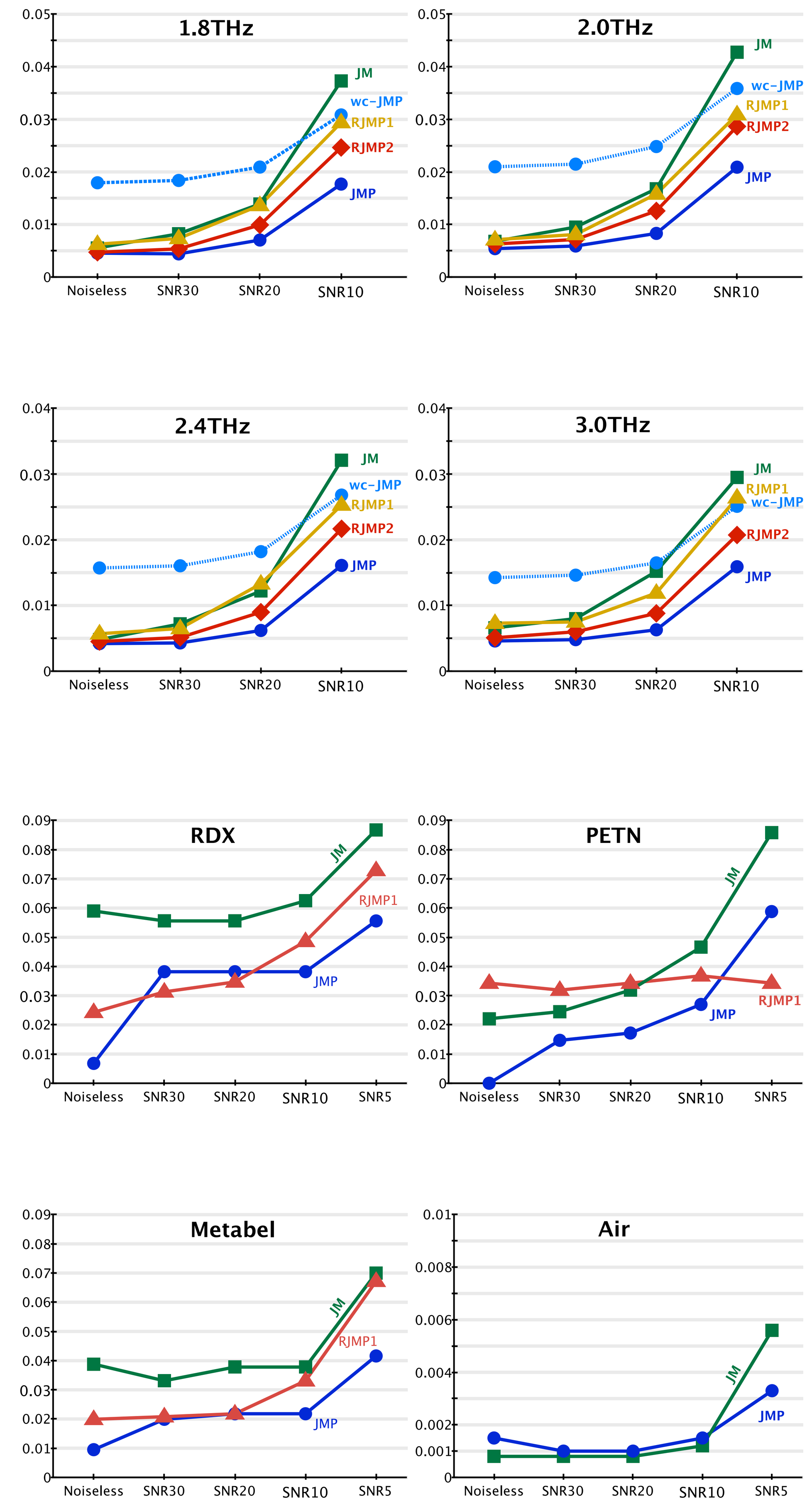

Exp1. Reconstruction
RJMP1 is given only spectra of RDX. wc-JMP and RJMP2 are given the worst-case spectral priors under 5% uncertainty.

Exp2. Recognition
pixel-wise labeling j at $\boldsymbol{r}$:
JM:minimizer of Euclidean distance from x to $\mathcal{E}_j$.
JMP: maximizer ν_j.
RJMP1: maximizer ν_j for small x^c

Discussion

- JMP: force spectral and spatial consistency during inversion; sensitive to the completeness and accuracy of spectral priors
- RJMP1: encourage sparse representation using given spectral priors
- RJMP2: : minimax optimization techniques
- Future work: handle uncertainties in accuracy and completeness at the same time